

Fast and Simple Preparation of Supercapacitor with CoMoO₄ as Electrode and Study of Its Photocatalytic Performance

Wang, Jing* ; Wang, Gang

School of Light Industry, Harbin University of Commerce, Harbin, P.R. CHINA

Hao, Jian

State Key Laboratory of High-efficiency Utilization of Coal and Green Chemical Engineering, Ningxia University, Ningxia, P.R. CHINA

Wang, Shen

MIT Key Laboratory of Critical Materials Technology for New Energy Conversion and Storage, School of Chemistry and Chemical Engineering, Harbin Institute of Technology, Harbin, P.R. CHINA

ABSTRACT : *In this paper, CoMoO₄ Porous NanoSheets (PNSs) were successfully fabricated on a carbon cloth substrate by a low-temperature water bath method. Through morphological characterization and phase analysis, the synthesized product is CoMoO₄ nanosheet, which has a porous structure with a diameter of about 400 nm and a thickness of about 100 nm. Through the electrochemical performance test, the synthesized product has good electrochemical performance. Under the condition of 1 A/g, the specific capacitance of CoMoO₄ PNSs is 1800 F/g, and after 10000 cycles of charging and discharging, the capacity maintenance rate is 99.6%. CoMoO₄ PNSs is a positive electrode, and activated carbon (AC) is a negative electrode. The device is assembled, and its theoretical voltage window reaches 1.6 V. After 8000 cycles of charging and discharging, the specific capacitance decreased from 121 F/g to 113 F/g, retaining 93.38% capacitance. In addition, we further studied the photocatalytic degradation of dyes on the synthetic materials. The degradation rates of Methyl Orange (MO), Rhodamine B (RhB) and Congo red (CR) dyes were 94.2%, 98.1%, and 96.4%, respectively. We further explored the cyclic stability of the material for RhB dye degradation. After 5 cycles of testing, it was found that the stability is very good, and can maintain 98.6%. The excellent electrochemical and photocatalytic properties of CoMoO₄ PNSs are mainly attributed to the special porous sheet structure and CoMoO₄ material. This work provides a new strategy and method for preparing excellent electrode materials and photocatalyst materials.*

KEYWORDS: *Supercapacitor; Photocatalytic; Low-temperature water bath method; CoMoO₄*

INTRODUCTION

With the rapid development of science and technology,

the problem of energy shortage and environmental pollution is more and more serious, how to effectively

*To whom correspondence should be addressed.

+ E-mail: wangwangmayong@126.com

1021-9986/2023/8/2405-2417

13/\$/6.03

store energy and protect the environment is a problem that people have to face. Ultracapacitor is considered one of the most promising energy storage devices in the energy field because of its high-power density, fast charge and discharge, environmental protection, and long service life [1]. However, the energy density of ultracapacitors is relatively low, which greatly affects their practical application [2]. According to the energy density formula $E=1/2CV^2$. We can find that the energy density is directly related to the specific capacitance (C) and voltage window (V) [3]. The specific capacitance can be improved by designing and developing electrode materials with excellent performance [4]. In this paper, by adjusting the proportion and content of raw materials, and adjusting the reaction temperature and time, we successfully prepared porous CoMoO_4 nanosheets by water bath thermal method. In addition, by assembling asymmetrical supercapacitors using two different electrode materials, the voltage window can be enlarged, thus increasing the energy density. In addition, water pollution is one of the most important environmental problems, the reasonable use of material photocatalytic performance can effectively degrade pollutants in water. It not only effectively alleviates the energy shortage, but also effectively protects the environment [6]. Therefore, the development of electrode materials with high performance has become the focus of research all over the world.

CoMoO_4 is considered as a promising electrode material for energy storage devices because of its high conductivity, cycle stability, redox activity and good rate-multiplication property. However, its specific capacitance is not good enough. In order to improve the behavior of supercapacitors, it is crucial to improve the dynamics of ion and electron transport inside the electrode and at the electrode-electrolyte interface. At present, an effective method is to prepare active materials with multi-dimensional structures. Because they can provide a shorter diffusion path length for ions, thus obtaining a higher charge and discharge rate. For example, nanowires [7], nanoflower [8], nanoneedles [9], core-shell structure [10], etc. These special structures increase the specific surface area and reactive sites of the electrode material, which both improve the electrochemical performance of the material. Zhou et al. [11] successfully prepared CoMoO_4 nanosheets on nickel foam by a two-step water bath method. The modified material

has excellent high specific capacitance (1097 F/g at 1 A/g) and excellent cycle stability (97.5% after 2000 cycles). Wang et al. [12] successfully synthesized CoMoO_4 nanowire array by the water bath method. The specific capacity of the material reached 940F/g at the current density of 1A/g, with the material as the positive electrode and activated carbon (AC) as the negative electrode. The asymmetrical supercapacitor has a maximum voltage of 1.6 V, a high energy density (46.7 Wh/kg) and a power density (8000 W/kg). Wang et al. [13] successfully prepared CoMoO_4 nanowire on carbon cloth by a water bath method. The density of CoMoO_4/CC electrode was 2100 F/g at 1 A/g, and the CoMoO_4/CC electrode showed excellent cycling performance of 94.53% after 10000 cycles, with activated carbon (AC)/CC as the negative electrode. At the current density of 1 A/g, the high specific capacitance of 184 F/g, specific energy of 65.42 Wh/kg (specific power of 2880 W/kg), specific power of 12000 W/kg (specific energy of 40.18 Wh/kg) and performance of 94.29% after 10000 cycles are achieved. In addition, CoMoO_4 also has excellent photocatalytic performance, good stability, and high photocatalytic efficiency, and is widely used in the field of photocatalytic. Ma et al. [14] successfully prepared CoMoO_4 nanomaterials by water bath method and high-temperature calcination, which could almost completely degrade MB in 90 minutes without pH adjustment. In addition, the stability experiments show that CoMoO_4 catalyst has high stability and excellent reliability, and the removal rate is 80% even after using five accumulative cycles. Shaheen et al. [15] are ZnO- CoMoO_4 nanocomposites, which possess 95% excellent catalyst for methyl orange degradation in the aqueous environment within 10 min in the dark environment according to the sol-gel synthesis method. In addition, the cyclic stability of this material is also good.

In this paper, CoMoO_4 PNSs were synthesized by a low-temperature water bath method, by adjusting the proportion of raw materials, and controlling the reaction temperature and reaction time. Due to its unique open porous morphology, CoMoO_4 PNSs have excellent electrochemical performance and photocatalytic degradation efficiency. Under the condition of 1A/g, the specific capacitance value of CoMoO_4 PNSs reaches 1800F/g, and after 10000 cycles of charge and

discharge, the capacitance maintenance rate reaches 99.6%. The device was assembled with activated carbon (AC) and its theoretical voltage window reached 1.6V. The specific capacitance value decreases from 121F/g to 113F/g after 8000 cycles of charge and discharge, retaining 93.38% capacitance value. In addition, the photocatalytic performance of the material showed that MO, RhB and CR dyes had a good degradation effect of more than 94%, and the degradation rate of RhB even exceeded 98.1%. The cyclic stability of the material was as high as 98.6% after 5 cycles. This research has provided a new method for the preparation of CoMoO_4 with excellent electrochemical properties and photocatalyst performances.

EXPERIMENTAL SECTION

In the experiments, none of the reagents were further purified. Carbon cloth was used as the conductive substrate and was repeatedly cleaned with hydrochloric acid, ultrapure water. Nickel foam has many advantages, such as good electrical conductivity, high surface area and special porous structure. Because of the above advantages of nickel foam as substrate, it can catalyze water decomposition more efficiently at high current density. Therefore, we choose nickel foam as the conductive substrate in this paper.

Preparation of the CoMoO_4 PNSs

The materials used in the experiment are $\text{CoCl}_2 \cdot 6\text{H}_2\text{O}$ and $\text{Na}_2\text{MoO}_4 \cdot 7\text{H}_2\text{O}$. $\text{CoCl}_2 \cdot 6\text{H}_2\text{O}$ is produced by Henan Dongke Chemical Products Sales Co., LTD. The purity of the sample is 99.9%. $\text{Na}_2\text{MoO}_4 \cdot 7\text{H}_2\text{O}$ is produced by Changzhou Baiyundu Chemical Co., LTD. The purity of the product is 99.5%. Weigh 0.14 g $\text{CoCl}_2 \cdot 6\text{H}_2\text{O}$ and 0.15 g $\text{Na}_2\text{MoO}_4 \cdot 7\text{H}_2\text{O}$ solid powder and place them in a 100mL beaker. Measure 50 mL of deionized water into a 100 mL beaker, and continuously stir it with the magnetic force for 2 hours, so that the weighing mixture of $\text{CoCl}_2 \cdot 6\text{H}_2\text{O}$ and $\text{Na}_2\text{MoO}_4 \cdot 7\text{H}_2\text{O}$ powder is fully dissolved in ultrapultraprine water. Transfer the above-mentioned mixed solution to a 100ml stainless steel reactor, put the treated foam nickel substrate into it, screw the sealed reactor tightly and treat it at 90 °C for 8 h. After that, the product was prepared and cooled to room temperature. Finally, it was cleaned with ethanol and

deionized water for 3 times and dried at 80 °C for 4 h.

Preparation of the activated carbon (AC) electrode

In this paper, activated carbon (AC) is used as the anode material of supercapacitor. The preparation method is as follows: the Weigh 20 g sesame straw, put it into tubular furnace and pass nitrogen as protective gas for carbonization, keep it at 600 °C for 2 h. Weigh 20 g sesame straw, put it into tubular furnace and pass nitrogen as protective gas for carbonization, Keep it at 600 °C for 2 h. Then wash the charcoal powder with deionized water to neutralize. Then add 0.5 g KOH solid, 5 mL anhydrous ethanol and 30mL deionized water, stir and dissolve, then soak for 12 h; After drying, the samples were taken out and kept for 1h at 700 °C. Finally, 1 mol /L hydrochloric acid was washed with ultrasonic water for 0.5 h. Finally, the washed sample was dried at 80 °C for 3h to obtain the product.

Material characterization

Scanning electron microscopy (SEM, JEOL-6360Lv, Tokyo, Japan. the acceleration voltage is 10 kV and the magnification is 1000 times) and transmission electron microscopy (TEM, JEOL JEM-201, Tokyo, Japan, the acceleration voltage is 200 kV, the point resolution is 0.24 nm, and the line resolution is 0.14 nm) were used to test and characterize the morphology of the prepared samples. The degradation of organic dyes was determined by UV-vis spectroscopy (UV-Vis, Shimadzu UV-2700, Room temperature, the sample cell is 1cm×1cm×1cm quartz cell, the test wavelength range is 350~1100 nm, and the wavelength resolution is 1nm). CHI 660E electrochemical workstation (Shanghai Chenhua Instrument Co., Ltd., Shanghai, China, Standard three-electrode system at room temperature) was used to test the electrochemical properties of the materials. The phase structure of the material was analyzed by X-ray Diffraction (XRD, Aolong Y2000, Liaoning, China, Cu $K\alpha$, $\lambda = 0.15405$ nm) and Energy Dispersive Spectroscopy (EDS, INCA Energy X-MAX-50, the acceleration voltage is 15 kV, and the count rate is 3500~4000 cps). The specific surface area and pore size distribution of the materials were tested by nitrogen adsorption and desorption (ASAP2020, Mi-cromeritics, USA, the temperature is 77 K).

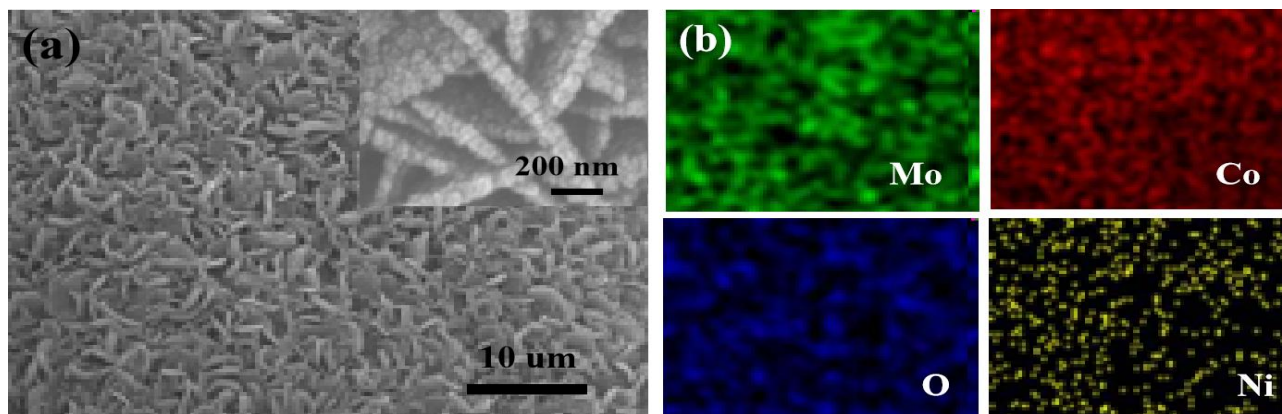


Fig. 1: (a) SEM images of CoMoO₄ Nanosheets and the inset is the magnified view; (b) SEM mapping images of Mo, O, and Ni elements, respectively

Electrochemical Test and Device assembly

The assembly of supercapacitors is composed of CoMoO₄ electrode, activated carbon electrode and PVA/KOH gel as electrolyte. The electrochemical performance of the device was tested in a two-electrode system with 2M KOH as electrolyte. The capacitance is calculated as follows:

$$C_s = i\Delta t / m\Delta V \quad (1)$$

$$E = 0.5C_s\Delta V^2 \quad (2)$$

$$P = 3600E/\Delta t \quad (3)$$

C_s (F/g) is the specific capacity. I (A) is the current density. ΔT (s) is the discharge time. ΔV (V) is the pressure drop during the discharge. M (g) is the mass of the active substance. Q is the amount of charge on the plate. P (W/Kg) is the power density. E (Wh/Kg) is the energy density.

Photocatalytic performance test

The photocatalytic performance of CoMoO₄ was tested as follows: The CoMoO₄ material was suspended in 300 mL RhB; MB and CR in aqueous solution (dye concentration 50 mg/L). It was stirred continuously for 120 min in the dark to ensure the adsorption-desorption equilibrium between the product and the dye. The solution was then placed under a 1500 W xenon lamp. The distance between the lamp and the liquid level is 15 cm. After irradiation, samples were taken every 10 min. After centrifugation at 1000 r/min, take the supernatant, and then use a UV-visible photometer to measure the change of the absorbance of the solution at a wavelength of 467 nm. The products were then separated by centrifugation, washed with deionized water, reused and

tested for cycle stability.

RESULTS AND DISCUSSION

CoMoO₄ was successfully prepared through our experiment, and then its surface appearance was observed by SEM. As shown in Fig. 1 (a), SEM images of CoMoO₄ were observed at low power. CoMoO₄ was evenly and densely arranged on the surface of the nickel foam, and it was found that the nickel base had been completely covered by it.

In Fig. 1 (a), the SEM image observed at high magnification is in the upper right corner. It is found that CoMoO₄ PNSs with a diameter of 100nm, are stacked on each other and form a porous structure, which is conducive to the improvement of electrochemical performance. TEM mapping was further conducted on the nickel foam as shown in Fig. 1 (b). It can be found that there are only four elements O, Co, Mo, and Ni, indicating that there are three elements O, Co, and Mo in the sample and no other impurity elements.

To get a closer look at the CoMoO₄ nanostructure, we tested it with TEM and as shown in Fig. 2 (a), we found that the nanosheets were closely distributed and stacked on each other to form a porous sheet structure. The area in the red box in Fig. 2 (a) was selected for the high-resolution test, and Fig. 2 (b) showed the crystal plane spacing of 0.34 nm respectively. The (002) crystal planes of CoMoO₄ PNSs electrode material are respectively corresponding to the corresponding selected electron diffraction test in the upper right illustration. It can be found that CoMoO₄ PNSs are a polycrystalline material. Fig. 2(c) shows the EDS test of this material. The results show that CoMoO₄ PNSs

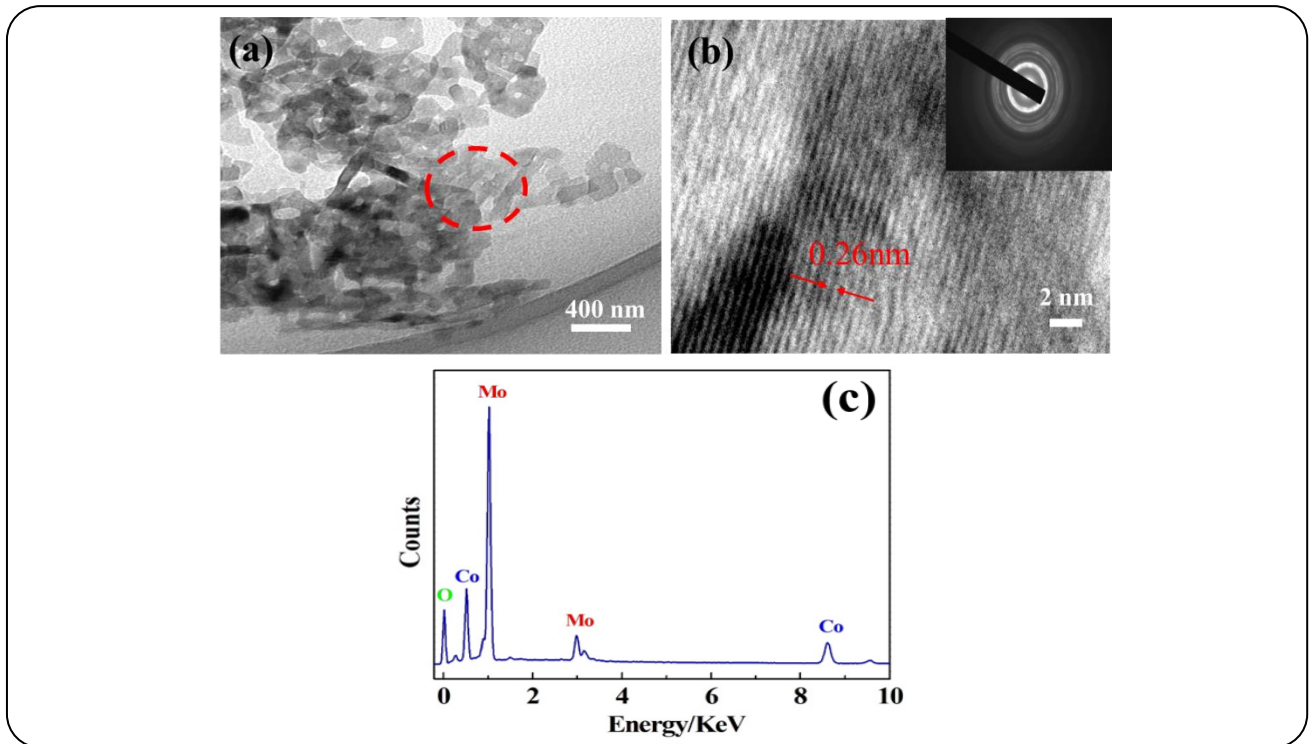


Fig. 2: (a) TEM image of the hybrid CoMoO_4 PNSs; (b) HRTEM image of CoMoO_4 Nanosheets and the inset is the corresponding SAED pattern; (c) EDS spectrum of CoMoO_4

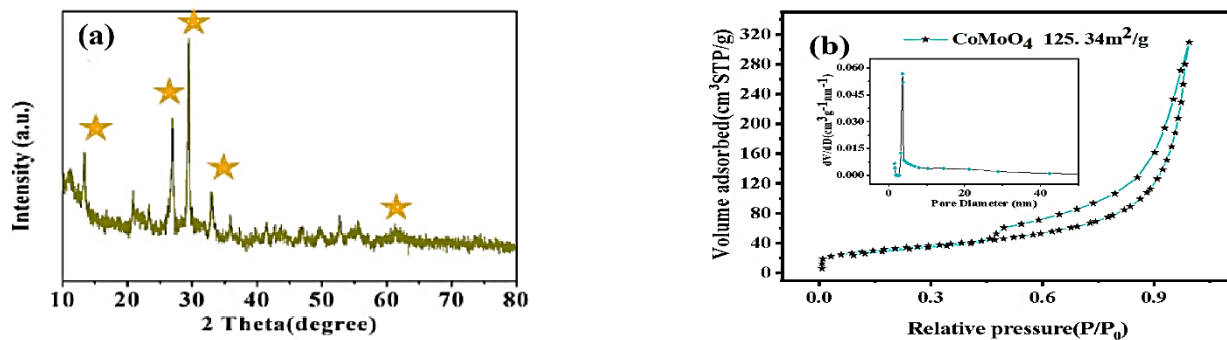


Fig. 3: (a) XRD patterns of CoMoO_4 PNSs; (b) N_2 adsorption/desorption curve of CoMoO_4 PNSs materials

only contains O, Co and Mo, which indicates that the prepared product is pure and does not contain other impurities.

Fig. 3(a) is XRD pattern of the material, which shows the crystal structure of CoMoO_4 PNSs. It is found that there are many peaks of high strength and few peaks of other impurities. The prepared product conforms to CoMoO_4 PNSs standard Card (JCPDS Card No. 21-0868) by test. The specific surface area of CoMoO_4 PNSs material prepared in the experiment was analyzed through nitrogen adsorption and desorption curve, as shown in Fig. 3 (b) The results show that the specific surface area of

CoMoO_4 PNSs nanocomposite is $125.34 \text{ m}^2/\text{g}$. The larger specific surface area is beneficial to the full diffusion of the electrode material in the electrolytic solution, thus shortening the transfer channel between electrolyte and electron, promoting the electrochemical reaction of the electrode material, and improving its electrochemical characteristics. The larger specific surface area is beneficial to the full diffusion of the electrode material in the electrolytic solution, thus shortening the transfer channel between electrolyte and electron, promoting the electrochemical reaction of the electrode material, and improving its electrochemical characteristics [17].

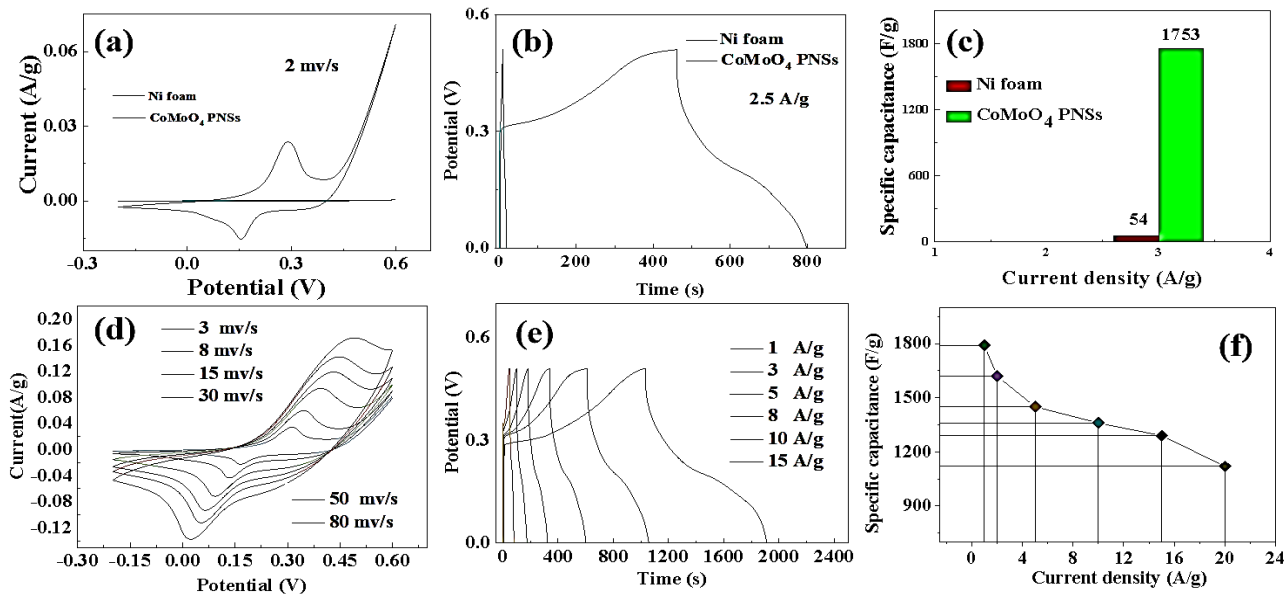


Fig. 4: (a) CV curves of the Ni foam and CoMoO₄ PNSs; (b) Charge and discharge of nickel foam and CoMoO₄ PNSs at the current density of 2.5 A/g; (c) Specific capacitance of CoMoO₄ PNSs and nickel foam at the current density of 3 A/g; (d) CV curves of CoMoO₄ PNSs at different scan rates; (e) Charge-discharge curves of CoMoO₄ PNSs at different current densities; (f) Specific capacitance of CoMoO₄ PNSs at varied current densities

In the experiment, the electrochemical properties of nickel foam and CoMoO₄ PNSs were analyzed as shown in Fig. 4 (a). As can be seen from the diagram, the area of the cyclic voltammetry curve of the nickel foam conductive substrate is smaller than that of the CoMoO₄ PNSs, which shows that the specific capacity of the nickel net can be neglected. Fig. 4 (b) is a constant current charge-discharge diagram of nickel foam, CoMoO₄ PNSs. Under the current density of 2.5 A/g, it is found that the discharge time of CoMoO₄ PNSs is much longer than that of pure nickel material, and the discharge time reaches 800 s. Therefore, the electrode of CoMoO₄ PNSs electrode material has better discharge properties than that of pure nickel material. As shown in Fig. 4 (c). According to the formula 1, the specific capacitance of a single electrode based on CoMoO₄ PNSs is 1753 F/g, while the specific capacitance of nickel foam is 54 F/g, and the specific capacitance value is only 1/32 of CoMoO₄ PNSs. Therefore, it is concluded that the influence of nickel foam on the capacitance of the supercapacitor is relatively small, while the influence of CoMoO₄ PNSs electrode is greater. Fig. 4 (d) shows the CV feature curves of CoMoO₄ PNSs at scanning speeds of 3, 8, 15, 30, 50 and 80 mV/s respectively. It can be seen that the peak current of all cyclic voltammetry curves increases linearly, and the

curve shape does not change greatly with the increase in sweep speed. This indicates that the electrochemical reaction rate is relatively fast, and the stability of the material is good. In order to test the rate performance of CoMoO₄ PNSs composite, charge and discharge tests were conducted under different current densities, as shown in Fig. 4 (e). It can be seen that each charge-discharge curve has a good symmetry, indicating that the material has a good reversible redox reaction behavior. According to Formula 1, we calculate the specific capacity under different current densities, as shown in Fig. 4 (f). With current densities of 1 A/g, 3 A/g, 5 A/g, 8 A/g, 10 A/g, and 15 A/g, the specific capacitance values of the materials could be as high as 1800 F/g, 1580 F/g, 1400 F/g, 1355 F/g, 1300 F/g and 1100 F/g, respectively. Showing excellent electrochemical performance.

Fig. (5) shows the charge-discharge cycle test diagram of CoMoO₄ PNSs electrode material at 2 A/g current density. It can be seen from the diagram that after 10000 cycles of charge-discharge, the specific capacitance value changes from 1639 F/g to 1633 F/g, retaining 99.6% capacitance value with a very small loss. It can be seen that CoMoO₄ PNSs electrode material has better charge-discharge cycle performance. Fig. 5 (b) shows the cyclic properties of the material under the condition that

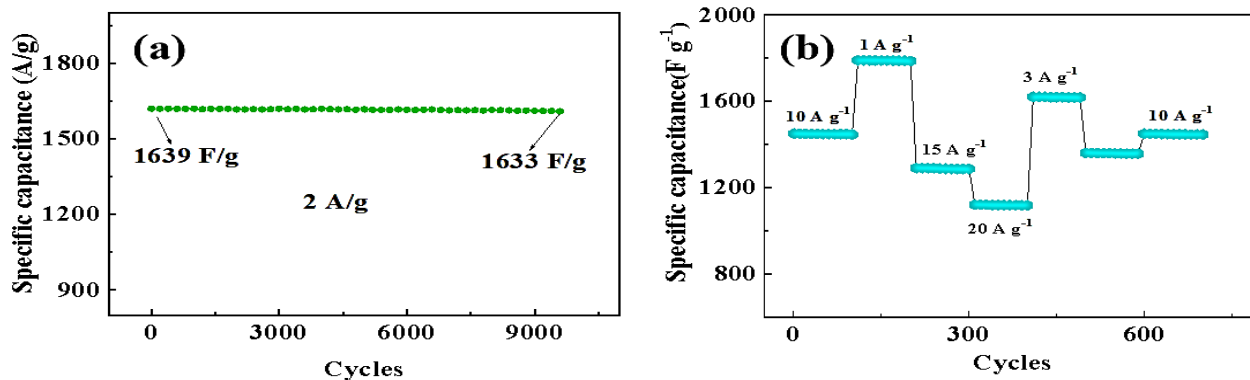


Fig. 5: (a) Cycle performance of CoMoO₄ PNSs for 10000 times at the current density of 2 A/g; (b) rate and cycle properties of CoMoO₄ PNSs at the different current densities

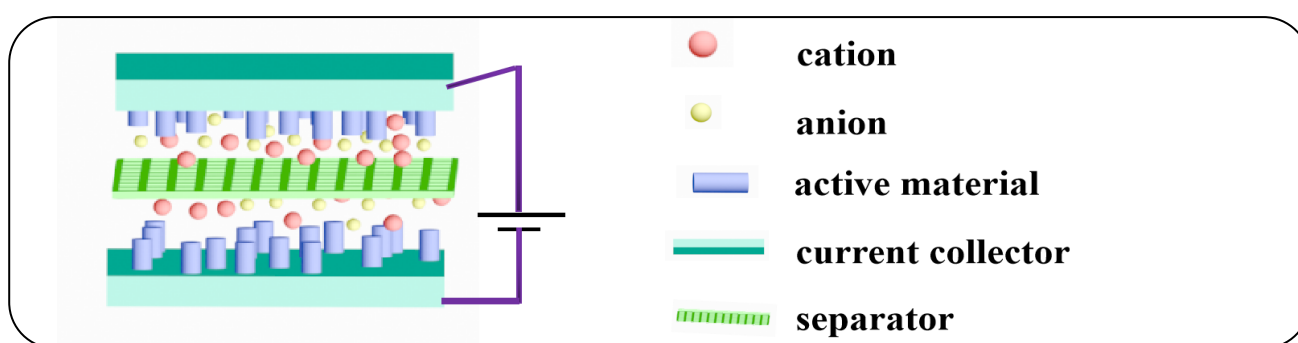


Fig. 6: The schematic mechanism of the supercapacitors device

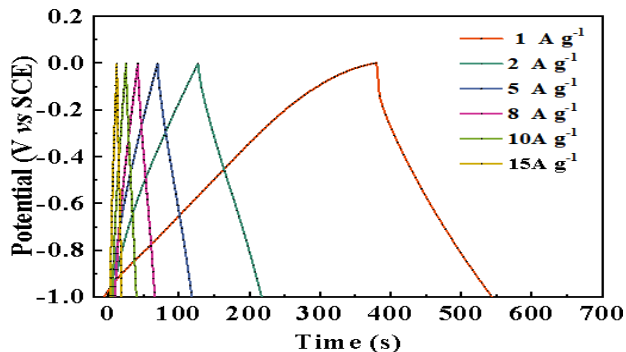


Fig. 7: Charge and discharge curves of AC at different current densities

the current density alternates 100 times and then returns to the initial same current density. When the charge-discharge density is 10 A/g, the structure shows a stable specific capacity of 1450 F/g for the first 100 cycles. In the following 600 cycles, although the current density changes in turn, the nanostructure always shows stable capacitance. When the current density is restored to 10 A/g, its area capacitance of 1442 F/g is almost unchanged compared with that of the initial same current density, indicating that the hybrid structure has excellent cycling stability. Asymmetric

electrochemical capacitor assembly: CoMoO₄//AC asymmetric device is prepared by CoMoO₄ PNSs electrode material as the positive electrode, Activated Carbon (AC) as the negative electrode, KOH as the electrolyte, adding a diaphragm between the positive electrode and the negative electrode. The charge between the CoMoO₄ PNSs Cathode and the AC anode was optimized before the device was assembled. The mass ratio of the two electrodes was calculated according to the specific capacitance and the potential window. Fig. 5 shows the charge-discharge curve at the negative emf window.

As can be seen from Fig. 7, with the increase of current density, charge and discharge time becomes shorter and the curves are roughly triangular, indicating that AC as electrode material has good charge and discharge reversibility and is suitable for the electrode material of supercapacitor.

Next, we explored the CV curves of CoMoO₄ PNSs and AC electrodes through experiments. As shown in Fig. 8, we plotted the CV characteristic curves of CoMoO₄ PNSs/CC and AC/CC electrodes at a scanning speed of 8 mV/s. In the Fig, it is not difficult to see that the highest

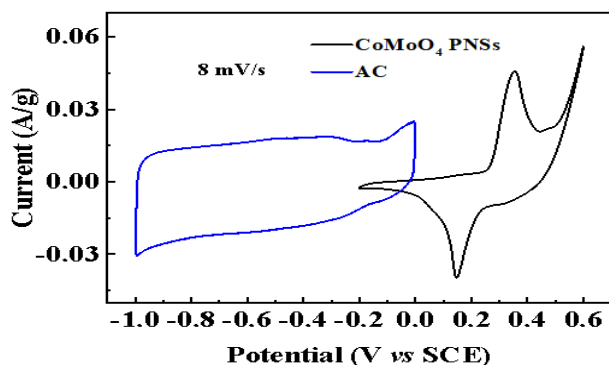


Fig. 8: (a) CV curves of the CoMoO₄ PNSs electrode and AC electrode performed a three-electrode cell in a 2 M KOH electrolyte at a scan rate of 8 mV/s

voltage of CoMoO₄ PNSs electrode is 0.6 V, and the lowest electrode voltage of AC electrode is -1.0 V. The voltage of the asymmetric device made of these two materials is the window value voltage of the difference between positive voltage and negative voltage, and its theoretical voltage window reaches 1.6 V.

Fig. 9 (a) shows the CV characteristic curves of CoMoO₄/AC devices at scanning speeds of 1, 5, 10, 20, 30 and 50 mV/s, respectively. It can be observed from the Fig. that at different scanning speeds, the overall shape of the current is roughly the same, and the current increases as the voltage increases. At different scanning speeds, the current reaches the highest at 1.6 V, and the voltage is concentrated in 0-1.6 V. ASC devices have relatively fast ion and electron transmission speed and excellent performance. As shown in Fig. 9 (b), the charge and discharge characteristic curves of ASC devices at different current densities of 1, 3, 5, 10, 15, 20 A/g are obtained. With the increase of current density, the discharge time becomes shorter. The potential voltage gradually increases from -1.0 to 0 and then decreases to -1. The characteristic curve is triangular, indicating that the electrochemical reversible performance and charge-discharge performance of ASC devices are excellent. Fig. 9 (c) shows that specific capacitance values of ASC devices tested at different current densities of 1, 3, 5, 10, 15 and 20 A/g are 131, 122, 113, 105, 86, 78 F/g, respectively. The electrochemical performance is excellent. Fig. (d) shows the test diagram of charge and discharge cycles of ASC devices. It can be seen from the diagram that after 8000 cycles of charge and discharge, the specific capacitance value decreases from 121 F/g to 113 F/g, retaining 93.38% capacitance value

and a very small loss. It can be seen that the performance of charge and discharge cycles of ASC devices is relatively good.

In the experiment, we further explore the photocatalytic principle and performance of CoMoO₄ PNSs. UV-Vis DRS was used to study the optical properties of the synthesized sample, and the optical absorption range of pure CoMoO₄ was about 467 nm. We calculated the bandgap position of CoMoO₄ by the Kubelka-Munk formula:

$$ah\nu=A(h\nu-E_g)^{n/2} \quad (4)$$

Where a , $h\nu$, A , and E_g are the absorption coefficient, discrete photon energy, constant, and band-gap width, respectively, while the n value is determined by the optical transition type of the semiconductor ($n=1$ for the direct transition and $n=4$ for the indirect transition). CoMoO₄ is an indirect transition semiconductor, so $n=4$. CoMoO₄ has a bandgap of 2.55 eV. The semiconductor valence band and conduction band potential can be calculated by the following formula:

$$E_{VB}=x-E^e+0.5E_g \quad (5)$$

$$E_{CB}=E_{VB} - E_g \quad (6)$$

Among them, E_{VB} is the edge potential of valence band (VB), E_{CB} is the edge potential of Conduction Band (CB), E_g is the band gap value of semiconductor material, E_e is the energy of free electrons on hydrogen element (about 4.5 eV), x is the electronegativity of semiconductor, which is defined as the geometric mean of absolute electronegativity of constituent atoms, and x value of CoMoO₄ is 5.01 eV. According to the above formula, the VB and CB potentials of CoMoO₄ can be calculated as 1.79 and -0.76 eV, respectively. The energy band structure of CoMoO₄ forms type II heterojunction, which is beneficial to the spatial separation of photogenerated electrons and photogenerated holes, reducing recombination efficiency and improving photocatalytic performance. When the energy of incident light is not less than the band gap, CoMoO₄ will stimulate electron e^- transition from valence band to conduction band, and also generate hole H^+ , which is the electron-hole pair 0. After that, the electrons and holes diffused to the surface of molybdate respectively, the holes had oxidizing ability, and the electrons had reducing ability, and the substances adsorbed on the surface of molybdate carried out redox

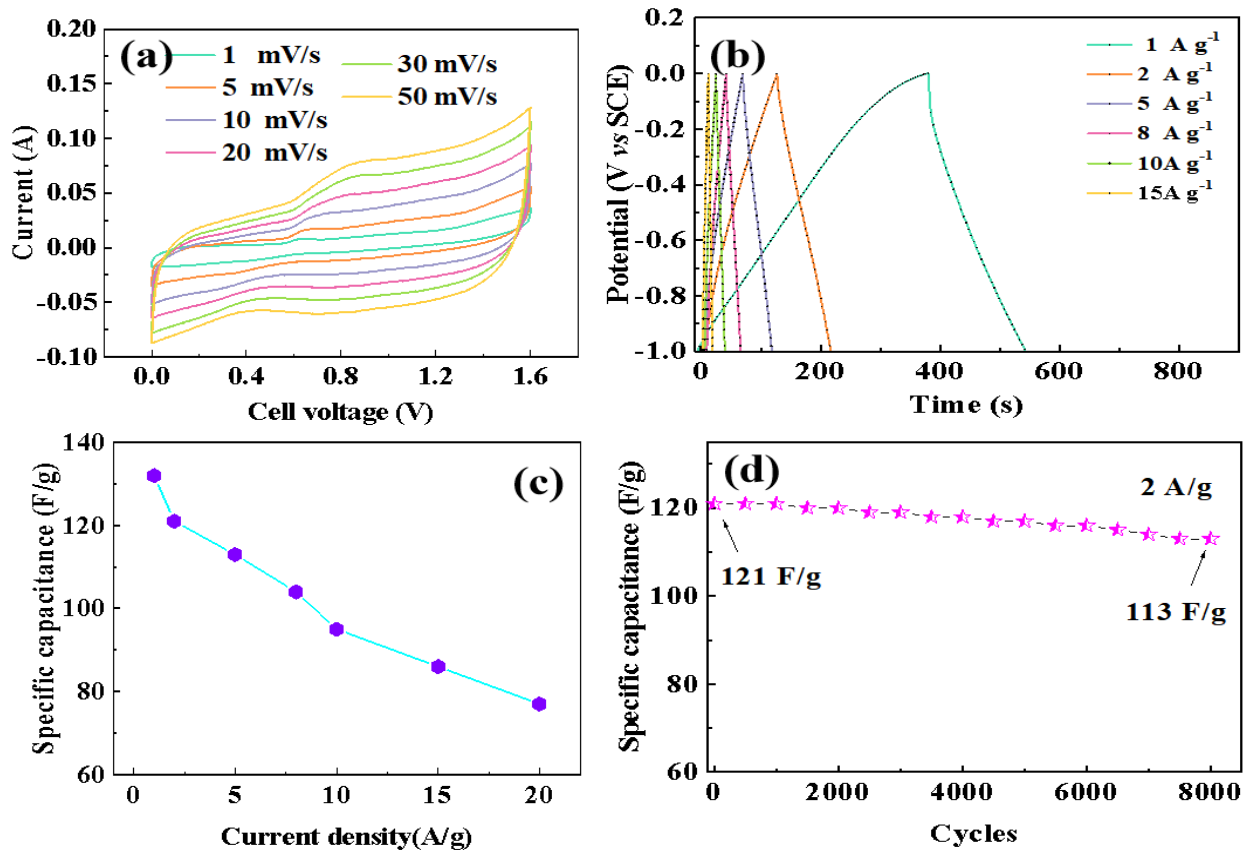


Fig. 9: (a) CV curves of CoMoO₄//AC ACS device at different scan rates; (b) Charge-discharge curves of CoMoO₄//AC ACS device at different current densities; (c) Specific capacitance of CoMoO₄//AC ACS device at varied current densities; (d) Cycling performance for 7000 times of the hybrid CoMoO₄//AC ACS device at a discharge current density of 1 A/g

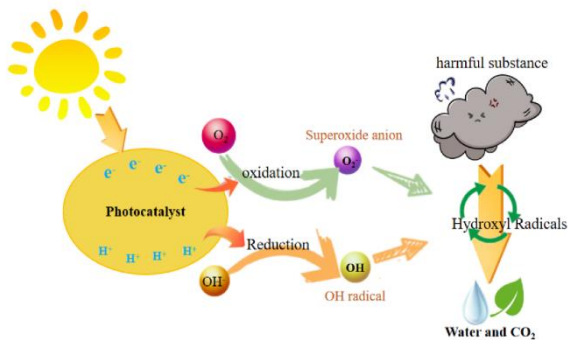


Fig. 10: Photocatalytic mechanism diagram

reaction to generate inorganic CO₂ and H₂O. The final product is very environmentally friendly, product as solid material, after the end of the reaction can be filtered for unified treatment, environmental protection, safety, economic, efficient. The chemical reaction equation is as follows:



In order to further study the photocatalytic performance of CoMoO₄, we explored the degradation experiment of CoMoO₄ PNSs nanomaterials on dyes such as MO, RhB, and CR. Fig. 6 (a, d, and g) is the photocatalytic reaction curve. (b, e, and h) is the Color change during the machination of different dyes. (c, f and i) is the Dye degradation rate curve. It can be seen from Fig. 9 (a-c, d-f, g-i) that CoMoO₄ PNSs degrade MO, RhB, and CR dyes by 90.2%, 98.1%, and 96.4%, respectively.

Fig. 9

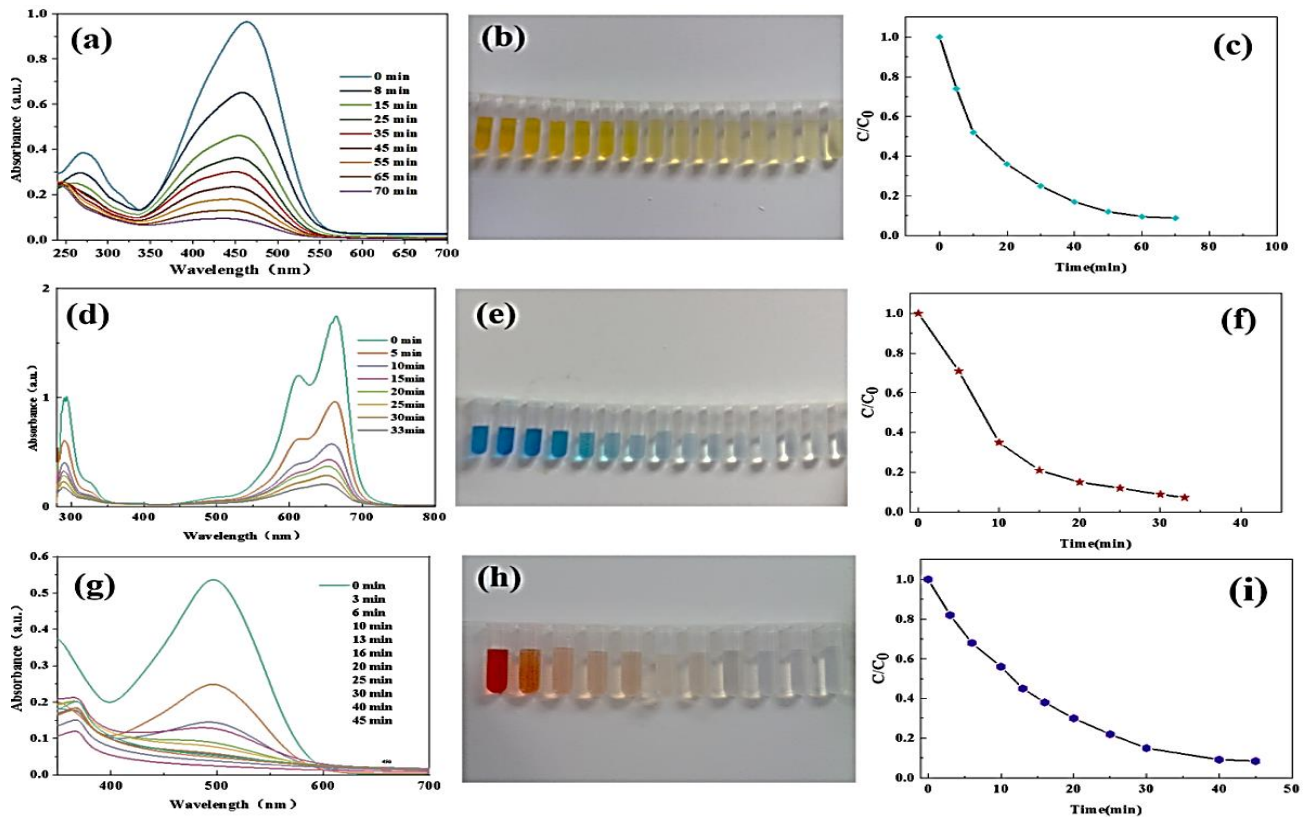


Fig. 9: photocatalytic degradation curves of different dyes (a) MO; (d) RhB; (g) CR. Color change during degradation of different dyes (b) MO; (e) RhB; (h) CR. Dye degradation rate curve; (c) MO; (f) RhB; (i) CR

(b, e, f) shows the color changes during the degradation process. It is obvious that CoMoO_4 PNSs has the degradation effect on all three dyes, but the degradation effect on RhB dye is the best, with the degradation rate as high as 98.1% in 33 minutes. Meanwhile, the degradation of MO, RhB, and CR by The Standard-Degussa /Evonik P25 was investigated. As shown in Fig. 10, it can be found that the degradation rates of MO, RhB, and CR by the Standard-Degussa/Evonik P25 are 85.1%, 82.6%, and 80.6%, respectively. According to the above data, it can be found that the photocatalytic performance of CoMoO_4 PNSs is far higher than that of the standard - Degussa / Evonik P25.

In order to further study the adsorption mechanism of MO, RhB, and CR by CoMoO_4 PNSs, the kinetics curves of photocatalytic degradation of the three dyes were analyzed. The Langmuir-Hinshelwood model is commonly used to analyze the kinetics of photocatalytic degradation of dyes, and the fitting equation is as follows [22]:

$$\ln \frac{C}{C_0} = kt \quad (15)$$

In the formula, C is the concentration of dye in solution at any time, C_0 is the initial concentration, and K is the first-order kinetic rate constant. The photocatalytic rate constants of CoMoO_4 PNSs prepared by the low-temperature water bath method for MO, RhB, and CR were 0.02325 min^{-1} , 0.02626 min^{-1} , and 0.02483 min^{-1} , respectively. The relevant data showed that the CoMoO_4 PNSs prepared by the hydrothermal method had a good catalytic performance for these three dyes.

The results of the above three dye degradation experiments show that the material has a better degradation effect on RhB. To further study the cyclic stability of the material, we studied the cyclic stability of the material to the dye RhB. The testing conditions were the same as the first dye degradation process. The results showed that the material was relatively stable in degrading dyes, and its cyclic stability reached 98.6%, which could be recycled 5 cycles without obvious changes, as shown in Fig. 11. This shows that the material has good cycle stability. We compared the research work with other materials, as shown in Table 1. In the process of photocatalytic reaction, the treatment of products are also

Table 1: Degradation efficiency of dyes by materials

material	pollutants	degradation time	degradation rate	ref
Ag ₂ O/g-CN/TiO ₂	RhB	60min	94.5%	23
Ag/BaTiO ₃	RhB	180min	96%	24
C@Co ₃ O ₄	RhB	20min	Near 90%	25
ZnO	CR	300min	>95%	26
ZnO-SnO ₂	MB	60min	96.53%	27
Nd-Gd Co-doped ZnO	MB	120min	93%	28
Bi ₂ WO ₆	RhB	100min	98%	29
ZnCo ₂ O ₄	CR	45min	96.2%	30
Degussa/Evonik P25	MO	33min	85.1%	this paper
CoMoO ₄ PNSs	RhB	33min	98.1%	this paper

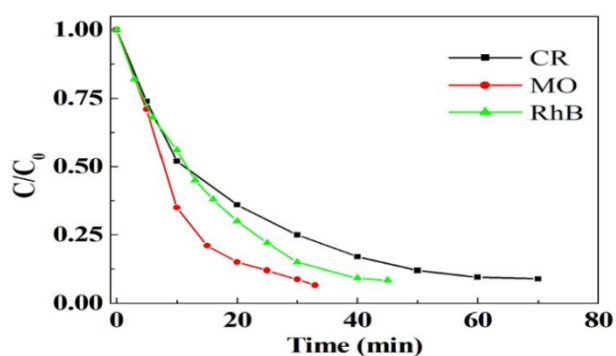


Fig. 10: Photocatalytic degradation curves of different dyes by The Standard-Degussa /Evonik P25

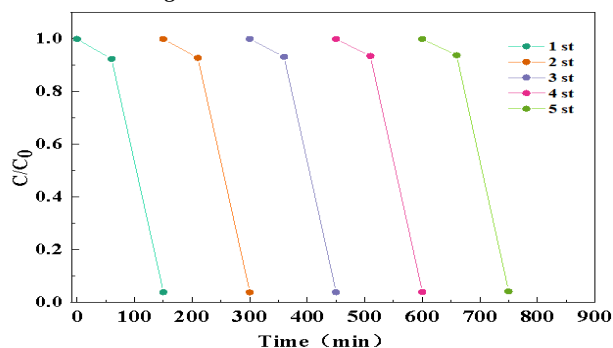


Fig. 11: Cycling properties of RhB for 5 cycles

very convenient. Organic dyes are almost oxidized and decomposed into water and carbon dioxide, and the products are treated as solid substances after filtration, which is very environmentally friendly and safe.

CONCLUSIONS

In summary, CoMoO₄ PNSs with excellent performance was prepared by the low-temperature water bath method. The prepared CoMoO₄ PNSs have excellent

electrochemical properties, and the specific capacitance value of CoMoO₄ PNSs reached 1800 F/g at 1 A/g. After 10,000 cycles of charging and discharging, the capacitance maintenance reached 99.6%. The theoretical voltage window of CoMoO₄ PNSs//AC reached 1.6 V. After 8000 cycles of charge and discharge, the capacitor retained 93.38% capacitance value. In addition, the degradation rates of MO, RhB, and CR dyes were also very good, all exceeding 94%. The degradation rate of RhB is 98.1%, and the stability of five cycles is 98.6%.

Funding

This research work was supported by the Young Scientific Research Item of Harbin University of Commerce (18XN034), the National Natural Science Foundation of China (no. 52002099), and the Foundation of State Key Laboratory of High-efficiency Utilization of Coal and Green Chemical Engineering (grant no. 2022-K74).

Received : Sep. 24, 2022 ; Accepted : Dec. 19, 2022

REFERENCES

- [1] Raza W., Ali F., Raza N., Luo Y., Kim K.H., Yang J., Kumar S., Mehmooda A., Kwon, E.E., [Recent Advancements in Supercapacitor Technology](#), *Nano Energy*, **52**: 441-473 (2018).
- [2] Najib S., Erdem E., [Current Progress Achieved in Novel Materials for Supercapacitor Electrodes: Mini Review](#), *Nanoscale Adv.*, **1(8)**: 2817-2827 (2019).
- [3] Ren B., Fan M., Zhang B., Wang J., [Novel Hollow NiO@Co₃O₄ Nanofibers for High-Performance Supercapacitors](#), *J. Nanosci. Nanotechnol.*, **18(10)**:

- 7004-7010 (2018).
- [4] Wei W, Chen Z, Zhang Y, Chen J., Wan L., Du C., Xie M., Guo X., Full-Faradaic-Active Nitrogen Species Doping Enables High-Energy-Density Carbon-Based Supercapacitor, *J. Energy Chem.*, **48**: 277-284 (2020).
- [5] Wu Z., Pu X., Ji X., Zhu Y., Jing M., Chen Q., Jiao F., High Energy Density Asymmetric Supercapacitors from Mesoporous NiCo₂S₄ Nanosheets, *Electrochim Acta*, **174**: 238-245 (2015).
- [6] Choudhary N., Li C., Moore J., Nagaiah N., Zhai L., Jung Y., Thomas J., Asymmetric Supercapacitor Electrodes and Devices, *Adv. Mater.*, **29**(21): 1605336 (2017).
- [7] Taylor C.M., Ramirez-Canon A., Wenk J., Mattia D., Enhancing the Photo-Corrosion Resistance of ZnO Nanowire Photocatalysts, *J. Hazard. Mater.*, **378**: 120799 (2019).
- [8] Dumrongrojthanath P., Thongtem T., Phuruangrat A., Thongtem, S., Synthesis and Characterization of Hierarchical Multilayered Flower-Like assemblies of Ag Doped Bi₂WO₆ and Their Photocatalytic Activities, *Superlattices Microstruct.*, **64**, 196-203 (2013).
- [9] Yayapao O., Thongtem T., Phuruangrat A., Thongtem S., Ultrasonic-Assisted Synthesis of Nd-Doped ZnO for Photocatalysis. *Mater. Lett.*, **90**, 83-86 (2013).
- [10] Wang R., Yang E., Qi X., Xie R., Qin S., Deng C., Zhong W., Constructing and Optimizing Core@Shell Structure CNTs@MoS₂ Nanocomposites as Outstanding Microwave Absorbers, *Appl. Surf. Sci.*, **516**: 146159 (2020).
- [11] Zhou E., Tian L., Cheng Z., Fu C., Design of NiO Flakes@CoMoO₄ Nanosheets Core-Shell Architecture on Ni Foam for High-Performance Supercapacitors, *Nanoscale Res. Lett.*, **14**(1): 1-11 (2019).
- [12] Wang J., Chang J., Wang L., Hao J., One-Step and Low-Temperature Synthesis of CoMoO₄ Nanowire Arrays on Ni Foam for Asymmetric Supercapacitors, *Ionics*, **24**(12): 3967-3973 (2018).
- [13] Wang J., Wang C., Wang S., Wang J., Cao W., Wang Z., CoMoO₄ Nanoneedles/Carbon Cloth for High-Performance Supercapacitors: Maximizing Mass Loading by Reaction Time. *Chemistry Select*, **6**(24): 6159-6167 (2021).
- [14] Ma T., Wu Y., Liu N., Tao X., Wu Y., Iron-Doped g-C₃N₄ Modified CoMoO₄ as an Efficient Heterogeneous Catalyst to Activate Peroxymonosulfate for Degradation of Organic Dye, *J. Disper. Sci. Technol.*, **43**(1): 80-93 (2021).
- [15] Shaheen I., Ahmad K.S., Thomas A.G., Compeán-González C.L., Jones R., Malik, M.A., Synthesis and Analysis of ZnO-CoMoO₄ Incorporated Organic Compounds for Efficient Degradation of azo Dye Pollutants under Dark Ambient Conditions, *Appl. Organomet. Chem.*, **34**(9): e5733 (2020).
- [16] Lijuan K., Yongqiang Y., Ruiyi L., Zaijun, L., Phenylalanine-Functionalized Graphene Quantum Dot-Silicon Nanoparticle Composite as an Anode Material for Lithium Ion Batteries with Largely Enhanced Electrochemical Performance, *Electrochim Acta*, **198**: 144-155 (2016).
- [17] Jiao Y., Pei J., Chen D., Yan C., Hu Y., Zhang Q., Chen G., Mixed-Metallic MOF Based Electrode Materials for High Performance Hybrid Supercapacitors, *J. Mater. Chem. A*, **5**(3): 1094-1102 (2017).
- [18] Sankar K.V., Lee S.C., Seo Y., Ray C., Liu S., Kundu A., Jun S.C., Binder-Free Cobalt Phosphate One-Dimensional Nanograsses as Ultrahigh-Performance Cathode Material for Hybrid Supercapacitor Applications, *J. Power. Sources.*, **373**: 211-219 (2018).
- [19] Pirhashemi M., Habibi-Yangjeh A., Facile Fabrication of Novel ZnO/CoMoO₄ Nanocomposites: Highly Efficient Visible-Light-Responsive Photocatalysts in Degradations of Different Contaminants, *J. Photoch. Photobio. A*, **363**: 31-43 (2018).
- [20] Feizpoor S., Habibi-Yangjeh A., Yubuta K., Vadivel S., Fabrication of TiO₂/CoMoO₄/PANI Nanocomposites with Enhanced Photocatalytic Performances for Removal of Organic and Inorganic Pollutants under Visible Light, *Mater. Chem. Phys.*, **224**: 10-21 (2019).
- [21] Yayapao O., Thongtem T., Phuruangrat A., Thongtem S., Sonochemical Synthesis of Dy-Doped ZnO Nanostructures and Their Photocatalytic Properties, *J. Alloys. Compd.*, **576**, 72-79 (2013).
- [22] Feizpoor S., Habibi-Yangjeh A., Yubuta K., Vadivel S., Fabrication of TiO₂/CoMoO₄/PANI Nanocomposites with Enhanced Photocatalytic Performances for Removal of Organic and Inorganic Pollutants under Visible Light, *Mater. Chem. Phys.*, **224**, 10-21 (2019).

- [23] Rajendran R., Vignesh S., Sasireka A., Suganthi S., Raj V., Baskaran P., Shkir M., AlFaify S., [Designing Ag₂O Modified g-C₃N₄/TiO₂ Ternary Nanocomposites for Photocatalytic Organic Pollutants Degradation Performance under Visible Light: Synergistic Mechanism Insight](#), *Colloid Surface A*, **629**: 127472 (2021).
- [24] He Z., Yu P., Wang H., Gao J., Zhao Y., Zhang H., Zhao Y., Miao Z., [Surface Plasmon Resonance-Induced Ag-BaTiO₃ Composites for Catalytic Performance](#), *J. Am. Ceram. Soc.*, **104(9)**: 4389-4397 (2021).
- [25] Liang J., Fu L., [Activation of Peroxymonosulfate \(PMS\) by Co₃O₄ Quantum Dots Decorated Hierarchical C@Co₃O₄ for Degradation of Organic Pollutants: Kinetics and Radical-Nonradical Cooperation Mechanisms](#), *Appl. Surf. Sci.*, **563**: 150335 (2021).
- [26] Deebansok S., Amornsakchai T., Sae-ear P., Siriphannon P., Smith S.M., [Sphere-Like and Flake-Like ZnO Immobilized on Pineapple Leaf Fibers as Easy-to-Recover Photocatalyst for the Degradation of Congo Red](#), *J. Environ. Chem. Eng.*, **9(2)**: 104746 (2021).
- [27] Lin J., Luo Z., Liu J., Li P., [Photocatalytic Degradation of Methylene Blue in Aqueous Solution by Using ZnO-SnO₂ Nanocomposites](#), *Mat. Sci. Semicon. Proc.*, **87**: 24-31 (2018).
- [28] Akhtar J., Tahir M.B., Sagir M., Bamufleh H.S., [Improved Photocatalytic Performance of Gd and Nd co-Doped ZnO Nanorods for the Degradation of Methylene Blue](#), *Ceram. Int.*, **46(8)**: 11955-11961 (2020).
- [29] Phuruangrat A., Maneechote A., Dumrongrojthanath P., Ekthammathat N., Thongtem S., Thongtem T., [Effect of pH on Visible-Light-Driven Bi₂WO₆ Nanostructured Catalyst Synthesized by Hydrothermal Method](#), *Superlattices Microstruct.*, **78**: 106-115 (2015).
- [30] Wang J., Wang G., Wang S., Hao J., Liu B., [Preparation of ZnCo₂O₄ Nanosheets Coated on Evenly Arranged and Fully Separated Nanowires with High Capacitive and Photocatalytic Properties by a One-Step Low-Temperature Water Bath Method](#), *Chemistry Select*, **7(13)**: e202200472 (2022).